Colloquia: LaThuile14

Measurement of the leptonic forward-backward asymmetry of top quark-antiquarks pairs in the dilepton channel with the D0 detector

A. Chapelain for the D0 Collaboration

CEA Saclay, IRFU/SPP - France

Summary. — We present measurements of forward-backward asymmetries of leptons produced in $t\bar{t}$ events in proton-antiproton collisions at the Fermilab Tevatron Collider. We consider final states where the $W^{\pm}$ bosons from top quark and antiquark decays both decay into $\ell\nu$ ($\ell = e, \mu$) resulting in oppositely charged dilepton inal states with accompanying jets. Using $9.7\,\text{fb}^{-1}$ of integrated luminosity collected with the D0 detector, we find the asymmetries in lepton pseudorapidity compatible with predictions based on the standard model.

PACS `14.65.Ha` – Top quarks.
PACS `12.38.Qk` – Experimental tests.
PACS `11.30.Er` – Charge conjugation, parity, time reversal, and other discrete symmetries.
PACS `13.85.Qk` – Inclusive production with identified leptons, photons, or other nonhadronic particles.

1. – Introduction

At next-to-leading order for the process $q\bar{q} \to t\bar{t}$, quantum chromodynamics (QCD) predicts that within the partonic rest frame the top quark is emitted preferentially in the direction of the incoming quark, while the top antiquark in the direction of the incoming antiquark. It comes mainly from the interference between $q\bar{q} \to t\bar{t}$ tree diagram with the NLO box diagram, and from the interference of initial and final state radiations ($q\bar{q} \to t\bar{t}g$). In the Standard Model (SM), the size of this asymmetry was computed a decade ago to be around 5% at the Tevatron [1] and 9% for the most recent computation including electroweak corrections [2].

Results released in 2011-2012 by the CDF and D0 Collaborations [3-5] have driven a lot of attention because some of the measured asymmetries were significantly higher than the SM predictions (see fig. 1 for the summary of the different inclusive asymmetry
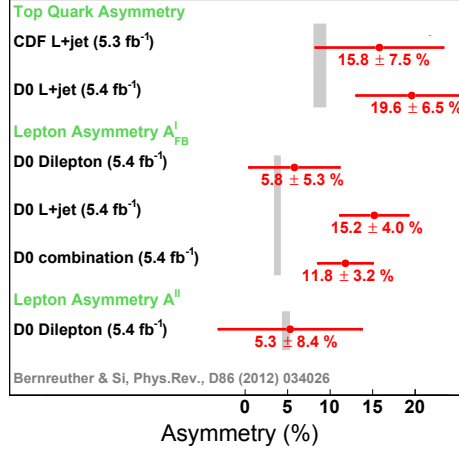
Fig. 1. – Summary of the differement inclusive asymmetry measurements performed at the Tevatron in 2012.

measurements performed at the Tevatron in 2012). It is therefore particularly interesting to look at the asymmetry with the full set of Tevatron data.

In this note, we report a new measurement [6] of the forward-backward asymmetry of leptons produced in $t\bar{t}$ events in the dilepton channel, based on all the data collected by the D0 Collaboration in Run II of the Tevatron corresponding to an integrated luminosity of $9.7\,\mathrm{fb}^{-1}$ following relevant data quality selection, and we compare our results with the most recent predictions based on the standard model [2]. We use the two observables $q \times \eta$ and $\Delta\eta$, where q and η are the charge and pseudorapidity of the lepton, and $\Delta\eta = \eta_{\ell^+} - \eta_{\ell^-}$ is the difference in lepton pseudorapidities. The pseudorapidity η is defined as a function of the polar angle θ with respect to the proton beam as $\eta = -\ln(\tan\frac{\theta}{2})$. Positive (negative) η corresponds to a particle produced in the direction of the incoming proton (antiproton). The single-lepton asymmetry A_{FB}^{ℓ} and dilepton asymmetry $A^{\ell\ell}$ are defined as

$$(1) \quad A_{\mathrm{FB}}^{\ell} = \frac{N(q \times \eta > 0) - N(q \times \eta < 0)}{N(q \times \eta > 0) + N(q \times \eta < 0)}, \qquad A^{\ell\ell} = \frac{N(\Delta\eta > 0) - N(\Delta\eta < 0)}{N(\Delta\eta > 0) + N(\Delta\eta < 0)},$$

where N corresponds to the number of leptons satisfying a given set of selection criteria. The A_{FB}^{ℓ} and $A^{\ell\ell}$ asymmetries are highly correlated as we discuss in sect. **7**.

2. – The D0 detector

The D0 detector [7-9] has a central tracking system consisting of a silicon microstrip tracker and a central fiber tracker, both located within a 2 T superconducting solenoidal magnet, with designs optimized for tracking and vertexing at detector pseudorapidities (relative to the center of the D0 detector) of $|\eta_{det}| < 3$ and $|\eta_{det}| < 2.5$, respectively. A liquid-argon sampling calorimeter has a central section (CC) covering pseudorapidities $|\eta_{det}|$ up to ≈ 1.1, and two end calorimeters (EC) that extend coverage to $|\eta_{det}| \approx 4.2$, with all three housed in separate cryostats [10]. An outer muon system, at $|\eta_{det}| < 2$,

TABLE I. – *Numbers of total expected (N_{expected}) and observed (N_{observed}) events from backgrounds and $t\bar{t}$ signal assuming the SM cross section (7.45 pb for a top quark mass of $m_t = 172.5$ GeV [19]). Expected numbers of events are shown with their statistical uncertainties.*

	$Z \to \ell\ell$	Dibosons	Multijet and W+jets	$t\bar{t} \to \ell\ell jj$	N_{expected}	N_{observed}
ee	$17.2^{+0.6}_{-0.6}$	$2.4^{+0.1}_{-0.1}$	$4.7^{+0.4}_{-0.4}$	$127.8^{-1.4}_{-1.4}$	$152.1^{+1.6}_{-1.6}$	147
$e\mu$ 2 jets	$13.7^{+0.5}_{-0.5}$	$3.9^{+0.2}_{-0.2}$	$16.3^{+4.0}_{-4.0}$	$314.7^{+1.1}_{-1.1}$	$348.6^{+4.2}_{-4.2}$	343
$e\mu$ 1 jet	$8.7^{+0.6}_{-0.6}$	$3.4^{+0.2}_{-0.2}$	$2.9^{+1.7}_{-1.7}$	$61.7^{+0.5}_{-0.5}$	$76.7^{+1.9}_{-1.9}$	78
$\mu\mu$	$17.5^{+0.6}_{-0.6}$	$1.9^{+0.1}_{-0.1}$	$0.0^{+0.0}_{-0.0}$	$97.7^{+0.6}_{-0.6}$	$117.1^{+0.8}_{-0.8}$	114

consists of a layer of tracking detectors and scintillation trigger counters in front of 1.8 T toroids, followed by two similar layers after the toroids [11].

3. – Simulation and backgrounds

Monte Carlo (MC) events are processed through a GEANT-based [12] simulation of the D0 detector. To simulate effects from additional overlapping $p\bar{p}$ interactions, "zero bias" events are selected randomly in collider data and overlaid on the fully simulated MC events. $t\bar{t}$ events are generated with the NLO generator MC@NLO [13, 14] interfaced with HERWIG [15] for parton showering and hadronization. Electroweak backgrounds as Drell-Yan process associated with jets and diboson production are simulated using ALPGEN [16] interfaced with PYTHIA [17] and PYTHIA alone respectively. Drell-Yan and diboson processes are normalized to their NNLO and NLO cross section, respectively. The so-called instrumental background arises mainly from multijets and W+jets events in which one or two jets are misidentified as electrons or where muons or electrons originating from the semileptonic decay of a heavy flavor hadron appear isolated. This instrumental background is estimated direclty in the data by the mean of the "matrix method".

4. – Event selection

The selection of events follows the approach developped for the measurement of the $t\bar{t}$ cross section in the dilepton channel at D0 [18]. We require at least two high p_T isolated leptons and missing energy due to the two neutrinos escaping the detection. We define three channels requiring at least two jets: dielectron channel (ee) with two electrons, electron-muon channel ($e\mu$ 2 jets) with one electron and one muon, and dimuon channel ($\mu\mu$) with two muons. We define an additional channel requiring exactly one jet, one electron and one muon ($e\mu$ 1 jet). We use the full angular coverage of the different part of the detector excluding the region between the calorimeter cryostats. The final selection is performed in two dimensions using information from the b-quark identification discriminant and the topological variables such as $H_T = p_T^{lepton} + \sum_{i=1}^{2} p_T^{jet}$ or the significance in missing tranverse energy $\mathcal{S}(\not{E}_T)$. The numbers of predicted background events, as well as the expected numbers of signal events, in the four channels are given in table I and show high signal purity of the selected sample.
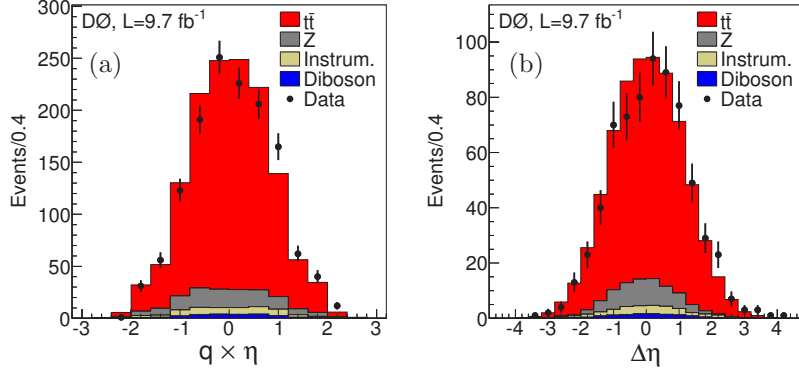
Fig. 2. – Distributions in (a) $q \times \eta$ and (b) $\Delta\eta = \eta_{\ell^+} - \eta_{\ell^-}$, for the sum of ee, $e\mu$ and $\mu\mu$ channels, along with predictions of the backgrounds and $t\bar{t}$ signal. The black points show data events and the error bars indicate the statistical uncertainty on the data.

5. – Measurements

Figure 2 presents the $q \times \eta$ and $\Delta\eta$ distributions for dilepton events after applying the event selection. To measure A_{FB}^{ℓ} and $A^{\ell\ell}$ we first restrict the distributions to the so-called visible phase space (or fiducial region). This region is defined such as the statistical uncertainty of the asymmetry within the full phase space is minimized using ensemble of pseudo datasets: $|\eta| < 2.0$ and $|\Delta\eta| < 2.4$. Within each of the four channels we perform a bin-by-bin subtraction of the estimated background contributions to the data. We then correct bin-by-bin the background subtracted distribution for the selection efficiency to get back to the production level result using MC@NLO $t\bar{t}$ sample. Figure 3 shows the corrected distributions for data compared to the predictions from MC@NLO.

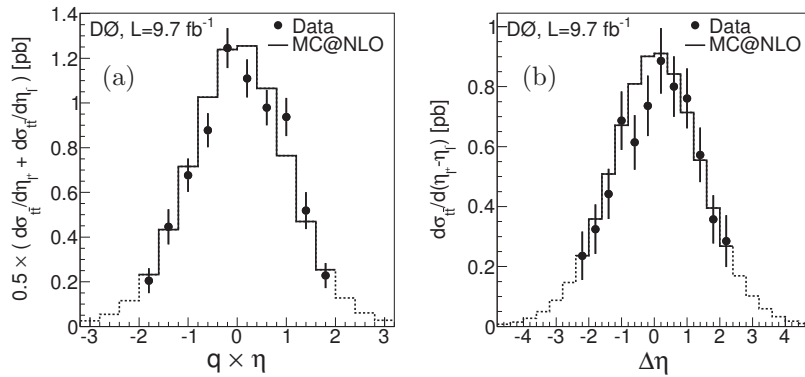Finally we extrapolate the measured production asymmetries from the visible phase

Fig. 3. – Distributions in (a) $q \times \eta$ and (b) $\Delta\eta$, for the combined ee, $e\mu$, and $\mu\mu$ channels after subtraction of background and correction for selection efficiency within the acceptance. The error bars indicate the statistical uncertainty on data. The dashed lines show the predictions from MC@NLO outside the analysis acceptance.

TABLE II. – *Systematic uncertainties for the asymmetries in the visible and full phase space. All values are given in %.*

	Visible phase space		Full phase space	
	A_{FB}^{ℓ}	$A^{\ell\ell}$	A_{FB}^{ℓ}	$A^{\ell\ell}$
Source				
Object ID	0.54	0.50	0.59	0.60
Background	0.66	0.74	0.72	0.88
Hadronization	0.52	0.62	0.62	0.92
MC statistics	0.19	0.23	0.23	0.37
Total	1.02	1.12	1.14	1.46

space to the full phase space by multiplying the asymmetries within the visible phase space with the calculated extrapolation factor, which is given by the ratio of the generator level SM $t\bar{t}$ asymmetries from MC@NLO without selections to asymmetries within the visible phase space ($|\eta| < 2$ and $|\Delta\eta| < 2.4$).

6. – Systematic uncertainties

Table II summarize the different systematic uncertainties we estimated. These systematic uncertainties are related to modeling of the background and the signal as well as instrumental uncertainty such as energy scale of jets and leptons. Further details about each category of uncertainty may be found in [6]. For the systematic uncertainties affecting the background, the background distributions are modified according to the systematic uncertainty and the background subtraction from data is done with the modified background distribution. The production-level asymmetry within the full phase space is then measured and the difference with the nominal measurement is taken as the value of the systematic uncertainty. For the systematic uncertainties affecting the signal, the selection efficiency correction is performed using a set of correction which includes the given systematic uncertainty and as for the background systematic uncertainties the difference between the nominal case and the shifted one is taken as the systematic uncertainty.

We also checked that the extrapolation procedure is consistent when using axigluon model instead of the standard model MC@NLO generator. These axigluon models [6, 20] can explain the large $t\bar{t}$ FB asymmetry measured by CDF and D0 being in the same time in agreement with experimental constraints from the Tevatron and the LHC.

7. – Results

We measure the asymmetry within the visible phase space for the different channels separately. We combine the four channels taking into account the correlations of the different systematic uncertainties using the BLUE method [21, 22]. Table III shows the combined result within the visible and the full phase space as well as the more recent predictions based on the standard model [2]. The measured A_{FB}^{ℓ} and $A^{\ell\ell}$ within the full phase space are consistent with the predictions. We perform diffentially the measurement

TABLE III. – *The measured asymmetries defined in eq. (1) for all channels combined within the visible and full phase spaces, compared to the predicted SM NLO asymmetries [2] for inclusive $t\bar{t}$ production. The measured asymmetry within the full phase space should be compared with the SM NLO prediction. The first uncertainty on the measured values corresponds to the statistical and the second to the systematic contribution. All values are given in %. The uncertainty on the SM NLO predictions are due to renormalization and factorization scale variations.*

	Visible phase space	Full phase space	Prediction
A_{FB}^{ℓ}	$4.1 \pm 3.5 \pm 1.0$	$4.4 \pm 3.7 \pm 1.1$	3.8 ± 0.3
$A^{\ell\ell}$	$10.5 \pm 4.7 \pm 1.1$	$12.3 \pm 5.4 \pm 1.5$	4.8 ± 0.4

of A_{FB}^{ℓ} and $A^{\ell\ell}$ in several bins of $|q \times \eta|$ and $|\Delta\eta|$ respectively as shown in the fig. 4. We do not observe significant dependence on these variables in the data and consistency with the MC@NLO predictions. The measurement in the data are also compared with the two models of axigluons. We do not put constraints on the models due to the large uncertainty on our measurement.

We measure the statistical correlation between A_{FB}^{ℓ} and $A^{\ell\ell}$ to be of 0.82 as explained in [6] in order to compute the ratio of these two asymmetries which allow to achieve a better sensitivity with ratio to the individual asymmetries due to systematic uncertainties cancellation. We measure a ratio equal to 0.36 ± 0.20 consistent at the level of 2 standard deviations with the prediction of 0.79 ± 0.10. The uncertainty on the theoretical ratio is estimated by adding in quadrature the uncertainty on the theoretical expectations for A_{FB}^{ℓ} and $A^{\ell\ell}$ and without taking into account the possible correlation between these two values. This predicted ratio is found to be almost the same for the different tested models as can be seen in fig. 5.

The D0 Collaboration measured A_{FB}^{ℓ} in the lepton+jets (ℓ+jets) final state within $|\eta| < 1.5$ to be $(4.2_{-3.0}^{+2.9})\%$ [23]. To enable a direct combination with the measurements in the ℓ+jets channel, the dilepton measurement is repeated using only leptons with
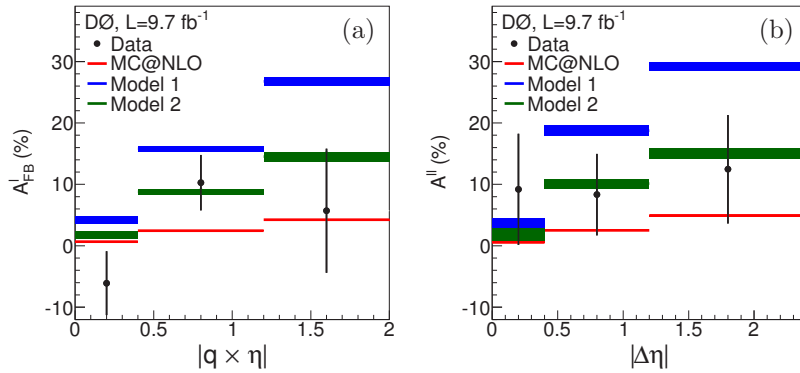

Fig. 4. – Asymmetry distributions in (a) $|q \times \eta|$ and (b) $|\Delta\eta| = |\eta_{\ell+} - \eta_{\ell-}|$, for the combined ee, $e\mu$, and $\mu\mu$ channels after background subtraction and after corrections for selection efficiency. The error bars indicate statistical uncertainties on the data. The data are compared with expectations from MC@NLO and axigluon Model 1 and Model 2.
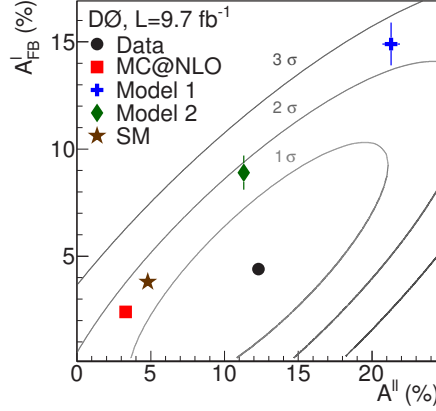
Fig. 5. – Extrapolated $A_{\rm FB}^{\ell}$ *versus* $A^{\ell\ell}$ asymmetries in $t\bar{t}$ data, the predictions from MC@NLO, axigluon models, and from the latest SM NLO prediction [2]. The ellipses represent contours of total uncertainty at 1, 2, and 3 SD on the measured result. All values are given in %. Predicted asymmetries are shown with their statistical uncertainties.

$|\eta| < 1.5$, finding $(4.3 \pm 3.5)\%$. The decrease in the statistical uncertainty is due to the removal of the events with $|\eta| > 1.5$, which have a large weight due to the acceptance corrections and thus increase the statistical uncertainty.

These two measurements which are in agreement were combined within the full phase space in order to take advantage of the full angular coverage of each channel. The result in the ℓ+jets channel was extrapolated with the same approach as the one used for the dilepton result. The two extrapolated results were combined with the BLUE method to take properly into account the correlations between the different systematic uncertainties. The result was found to be $(4.7 \pm 2.7)\%$.
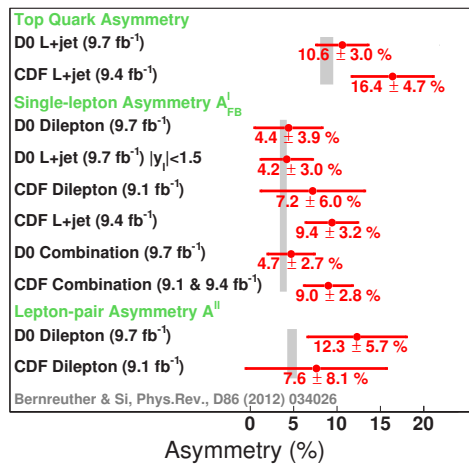

Fig. 6. – Summary of the differement inclusive asymmetry measurements performed at the Tevatron in 2014.

These results are in agreement with the results from the CDF Collaboration in the dilepton and ℓ+jets channels as well as their combination [24, 25]. Figure 6 summarize the measurement of the asymmetry from the Tevatron for both the $t\bar{t}$ and leptonic asymmetries. To summarize, measurements from the D0 Collaboration agree with the predictions based on the standard model [2] while measurments from the CDF Collaboration show deviations at the level of 2 standard deviations with the predictions. Moreover, the measurements from D0 agree with both the predictions and measurements from the CDF Collaboration, the situation is thus still puzzling. The combination of the CDF and D0 results will be the last step to build the legacy measurement from the Tevatron and discussions are currently ongoing to achieve this combination.

8. – Conclusion

We presented the measurement of the leptonic forward-backward asymmetry of top quark-antiquark pairs in the dilepton channel with the D0 detector. We found the asymmetry A^ℓ_{FB} and $A^{\ell\ell}$ to be in agreement with the predictions based on the standard model and the ratio $A^\ell_{\mathrm{FB}} A^{\ell\ell}$ to be in slight tension with the prediction at the level of two standard deviations. The A^ℓ_{FB} measurement was combined with the measurement performed in the ℓ+jets channel by the D0 Collaboration. The combined measurement was found to be in agreement with the prediction.

REFERENCES

[1] KÜHN J. H. and RODRIGO G., *Phys. Rev. Lett.*, **81** (1998) 49, http://link.aps.org/doi/10.1103/PhysRevLett.81.49.
[2] BERNREUTHER W. and SI Z.-G., *Phys. Rev. D*, **86** (2012) 034026.
[3] AALTONEN T. *et al.*, *Phys. Rev. D*, **87** (2013) 092002.
[4] ABAZOV V. M. *et al.*, *Phys. Rev. D*, **84** (2011) 112005.
[5] ABAZOV V. M. *et al.*, *Phys. Rev. D.*, **87** (2013) 011103(R).
[6] ABAZOV V. M. *et al.*, *Phys. Rev. D*, **88** (2013) 112002.
[7] ABAZOV V. M. *et al.*, *Nucl. Instrum. Methods Phys. Res. A*, **565** (2006) 463.
[8] ANGSTADT R. *et al.*, *Nucl. Instrum. Methods Phys. Res. A*, **622** (2010) 298.
[9] ABOLINS M. *et al.*, *Nucl. Instrum. Methods Phys. Res. A*, **584** (2008) 75.
[10] ABACHI S. *et al.*, *Nucl. Instrum. Methods Phys. Res. A*, **338** (1994) 185.
[11] ABAZOV V. M. *et al.*, *Nucl. Instrum. Methods Phys. Res. A*, **552** (2005) 372.
[12] BRUN R. and CARMINATI F., *CERN Program Library Long Writeup W5013 (1993)*, (unpublished).
[13] FRIXIONE S. and WEBBER B. R., *JHEP*, **06** (2002) 029.
[14] FRIXIONE S. and WEBBER B. R., arXiv:0812.0770 (2008).
[15] CORCELLA G. *et al.*, *JHEP*, **01** (2001) 010.
[16] MANGANO M. L. *et al.*, *JHEP*, **07** (2003) 001.
[17] SJOSTRAND T., MRENNA S. and SKANDS P. Z., *JHEP*, **05** (2006) 026.
[18] ABAZOV V. M. *et al.*, *Phys. Lett. B*, **704** (2011) 403.
[19] MOCH S. and UWER P., *Phys. Rev. D*, **78** (2008) 034003.
[20] FALKOWSKI A., MANGANO M. L., MARTIN A., PEREZ G. and WINTER J., *Phys. Rev. D*, **87** (2013) 034039.
[21] VALASSI A., *Nucl. Instrum. Methods Phys. Res. A*, **500** (2003) 391.
[22] LYONS L., GIBAUT D. and CLIFFORD P., *Nucl. Instrum. Methods Phys. Res. A*, **270** (1988) 110.
[23] ABAZOV V. M. *et al.* (D0 COLLABORATION), *Phys. Rev. D*, **90** (2014) 072001.
[24] AALTONEN T. A. *et al.* (CDF COLLABORATION), *Phys. Rev. Lett.*, **113** (2014) 042001.
[25] AALTONEN T. A. *et al.*, *Phys. Rev. D*, **88** (2013) 072003, http://link.aps.org/doi/10.1103/PhysRevD.88.072003.